Adaptive Combustion Regulation in Solid Fuel Ramjet

Parham Oveissi*, Ankit Goel†,
Department of Mechanical Engineering, University of Maryland, Baltimore County

Ozgur Tumuklu‡,
Department of Mechanical, Aerospace and Nuclear Engineering, Rensselaer Polytechnic Institute

Gohar T. Khokhar§, Kyle Hanquist¶
Department of Aerospace and Mechanical Engineering, University of Arizona

Control of the combustion process under hypersonic conditions remains a challenging problem. In this paper, we investigate the application of a data-driven, learning-based control technique to regulate a combustion process evolving inside a solid fuel ramjet to regulate the generated thrust under unknown operating conditions. A computational model to simulate the combustion dynamics is developed by combining compressible flow theory with equilibrium chemistry. The computational model is simulated to ascertain the combustion dynamics' stability and establish the engine's operational envelope. Based on retrospective cost optimization, an online learning controller is then integrated with the computational model to regulate the generated thrust. Numerical simulation results are presented to demonstrate the robustness of the adaptive control system.

I. Introduction

Due to their steady and extended-duration thrust, ramjet engines are particularly well-suited for long-range operation at high speeds. The lack of rotating turbomachinery makes the ramjet much simpler to design, operate, and maintain than other air-breathing propulsion systems. Based on the type of fuel used, ramjets can be classified as liquid-fuel (LFRJ) or solid-fuel (SFRJ) ramjets. Due to the lack of turbopumps, fuel bladders, injectors, and associated plumbing, an SFRJ is much simpler than a comparably-sized LFRJ. Due to solid fuel's higher volumetric energy density, the SFRJ has the potential for a greater range than the LFRJ. Additionally, since the combustion flame front spans the entire length of the fuel grain, SFRJs are less likely than LFRJs to suffer from combustion instabilities. Finally, SFRJ also has the advantage of being able to be stored as a "wooden round" without the usual logistical concerns associated with liquid fuels.

SFRJ development has been an active area of research for over four decades. Since the 1980s, several researchers have developed computational code to simulate the flow conditions inside an SFRJ [1–5]. These numerical simulations highlighted the complex flow interaction and qualitatively showed the response of an SFRJ in steady-state conditions. Recently, the JENRE framework has been used to simulate the flow in multi-physics problems [6–8]. In particular, JENRE was used to simulate unstart in a supersonic combustor [9].

A typical SFRJ geometry is shown in Figure 1. The lining of the combustor is the solid fuel grain. The high-speed, high-temperature flow vaporizes and ignites the fuel, adding energy to the flow and resulting in the generation of thrust. If the airflow rate is too low, heat addition might be insufficient to generate the necessary thrust, whereas if the flow rate is too high, the inlet may unstart due to excessive heat addition, or the combustion blowoff limits may be exceeded. Each of these scenarios can lead to flame extinction and loss of thrust. Therefore, the thermodynamic state (the pressure, temperature, and flow rate at the combustor) must be maintained within a relatively narrow range of operating conditions. Because of the complexity of the multi-physics processes involved (solid combustion, mixing, and high-speed flow), a stable operational range is extremely difficult to predict analytically. Reliable operation of SFRJ thus requires an approach that maintains the state of the SFRJ within acceptable limits and is robust to parametric variations and external disturbances over as wide an operating envelope as possible.

*Graduate Student, Department of Mechanical Engineering, 1000 Hilltop Circle, Baltimore, MD 21250.
†Assistant Professor, Department of Mechanical Engineering, 1000 Hilltop Circle, Baltimore, MD 21250.
‡Assistant Professor, Department of Mechanical, Aerospace and Nuclear Engineering, 110 Eighth Street | Troy, NY USA 12180.
§Postdoctoral Research Associate, Aerospace and Mechanical Engineering Department, Tucson, AZ 85721, AIAA Member.
¶Assistant Professor, Department of Aerospace & Mechanical Engineering, 1130 N. Mountain Avenue, University of Arizona, Tucson, AZ 85721, AIAA Senior Member.

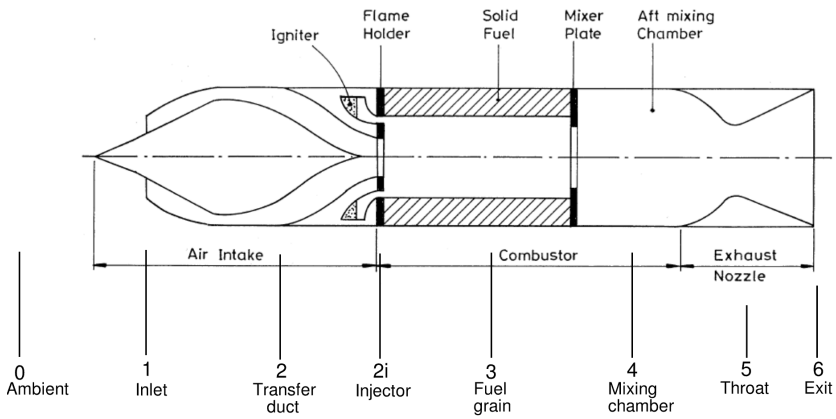

Fig. 1 A typical SFRJ cross section.

The current state-of-the-art for SFRJ thrust regulation uses passive and open-loop control strategies that involve the careful geometric design of the combustor and fuel grain. While these methods have achieved a limited amount of success, in order to make the most effective use of SFRJ-powered vehicles as a practical propulsion system for tactical applications, it is necessary to take advantage of advanced closed-loop control strategies to enable active thrust modulation required by optimal guidance strategies for complex missions. Unlike passive thrust modulation, where the thrust output of the SFRJ cannot be arbitrarily regulated during the mission, in an active closed-loop control strategy, the thrust would be regulated by an onboard control system that compensates for system uncertainties and adjusts the inputs accordingly to generate the thrust level required by the guidance law. Furthermore, instead of relying on a priori predictions of unstart, a data-driven control system can potentially identify unstart and adjust the control signal to arrest the engine unstart autonomously, thus maximizing the potential of the SFRJ engine.

In order to regulate the thrust generated by an SFRJ, several researchers developed and validated algebraic relations between the flow rate and the thrust generated by an SFRJ in static conditions using conservation of mass, momentum, and energy equations and quasi-static flow assumptions [2, 5, 10–13]. The effect of disturbances on the flow was considered in [14]. Importantly, these approaches rely on accurate knowledge of the physical parameters of the SFRJ. Inaccuracies in measurement propagate to incorrect input computation, and thus to incorrect thrust output. Furthermore, these static control laws were validated only in benign flow conditions.

In order to compensate for uncertainty and unmodeled physics, closed-loop control techniques to regulate the thrust generated by SFRJ were explored over the last two decades [15, 16]. In Ref. [15], the simplified ODE was used to develop an adaptive controller to regulate the thrust. However, the adaptive controller was validated only in simulation. Furthermore, the resulting control system was only demonstrated to regulate the output of the system as modeled by ODEs, not by the more realistic and physically motivated PDEs.

In our related recent work described in Refs. [17–19], we developed an adaptive control system to regulate the thrust and prevent inlet unstart in a liquid-fuel scramjet engine. The adaptive control system was based on retrospective cost optimization, where an auxiliary cost function, based on measured data and past inputs, is optimized to update the control law continually. This control technique, called retrospective cost adaptive control (RCAC), requires minimal modeling information. In most applications, a simple first-order transfer function, which can be easily obtained by open-loop system simulation or from experimentally collected data, is sufficient. Within the context of RCAC, this transfer function is called the *target model* since the RCAC algorithm updates the control law to drive an internal transfer function to the user-specified target model. It has been observed in numerous simulations and physical experiments that RCAC is insensitive to the choice of the target model. For example, the magnitude of the scalar that parameterizes the target model can be varied by as much as two orders of magnitude without adversely affecting the closed-loop performance. A key feature of RCAC that makes it particularly attractive to flow-control problems is its ability to adapt online. Furthermore, since RCAC requires only measured data and not a system model to optimize the controller, it can be directly integrated with a numerical simulation for training and stress-testing purposes. These features enable RCAC to be tuned using a computationally simple simulation of the system and then adapt appropriately to a more realistic simulation or the physical system itself.

In this work, we develop a computational model to simulate the multiphysics dynamics evolving in an SFRJ. Section

II describes the computational model in detail and the simplified SFRJ geometry used in this work. Section III describes the learning-based control system used to regulate the thrust of the SFRJ model and presents numerical simulation results to demonstrate the successful application of the adaptive control to regulate the SFRJ thrust. Finally, the paper concludes in Section IV with a summary of the paper and a discussion of the results.

II. Computational Modeling of SFRJ

The dynamic performance of SFRJ, including three-dimensional flow effects, viscous effects, and nonequilibrium chemistry, has been investigated using computational fluid dynamics techniques [4, 5, 20]. It is shown in [21–24] that all turbulent scales can be modeled with moderate computational cost and the capability to predict high-temperature/real gas effects with Reynolds Averaged Navier Stokes solvers (RANS). This work uses the SU2-NEMO (NonEquilibrium MOdels) code to RANS fidelity [25–27]. To model continuum hypersonic flows, SU2-NEMO solves the Navier-Stokes equations for multi-species gases in thermochemical nonequilibrium. As shown in [28], the governing equations can be expressed compactly in conservation form as

$$\mathcal{R}(\mathcal{U}, \nabla\mathcal{U}) = \frac{\partial \mathcal{U}}{\partial t} + \nabla \cdot \mathcal{F}^c(\mathcal{U}) - \nabla \cdot \mathcal{F}^v(\mathcal{U}, \nabla\mathcal{U}) - \mathcal{Q}(\mathcal{U}) = \mathbf{0}, \tag{1}$$

where the conservative variables ($\mathcal{U}$), convective fluxes ($\mathcal{F}^c$), viscous fluxes ($\mathcal{F}^v$), and source terms ($\mathcal{Q}$) are

$$\mathcal{U} = \begin{bmatrix} \rho_1 \\ \vdots \\ \rho_{n_s} \\ \rho\mathbf{u} \\ \rho e \\ \rho e^{ve} \end{bmatrix}, \quad \mathcal{F}^c = \begin{bmatrix} \rho_1\mathbf{u}^T \\ \vdots \\ \rho_{n_s}\mathbf{u}^T \\ \rho\mathbf{u}\mathbf{u}^T + P\mathcal{I} \\ \rho h\mathbf{u}^T \\ \rho e^{ve}\mathbf{u}^T \end{bmatrix}, \quad \mathcal{F}^v = \begin{bmatrix} -\mathbf{J}_1 \\ \vdots \\ -\mathbf{J}_{n_s} \\ \boldsymbol{\sigma} \\ \mathbf{u}^T\boldsymbol{\sigma} - \sum_k \mathbf{q}^k - \sum_s \mathbf{J}_s h_s \\ -\mathbf{q}^{ve} - \sum_s \mathbf{J}_s e_s^{ve} \end{bmatrix}, \quad \mathcal{Q} = \begin{bmatrix} \dot{\omega}_1 \\ \vdots \\ \dot{\omega}_{n_s} \\ \mathbf{0} \\ 0 \\ \dot{\Theta}^{tr:ve} + \sum_s \dot{\omega}_s e_s^{ve} \end{bmatrix} \tag{2}$$

where the number of species is denoted by n_s. The density, velocity, the total energy and vibrational energy per unit volume, pressure, enthalpy, the mass diffusion fluxes, the conduction heat flux for each thermal energy mode (k), and the viscous stress tensor are represented with ρ, u, e, e^{ve}, P, h, $\mathbf{J}$, $\mathbf{q}^k$, and $\boldsymbol{\sigma}$, respectively. Source terms expressing the volumetric production of each species are expressed as

$$\dot{\omega}_s = M_s \sum_r (\beta_{s,r} - \alpha_{s,r})(R_r^f - R_r^b), \tag{3}$$

where the reaction rates are modeled using an Arrhenius formulation and the forward and backward reaction rates for a given reaction r are R_r^f and R_r^b with the reaction exponents of $\alpha_{s,r}$ and $\beta_{s,r}$, respectively. Finally, the energy exchange between the translational-rotation and vibrational-electronic modes is modeled using a Landau-Teller formulation

$$\dot{\Theta}^{tr:ve} = \sum_s \rho_s \frac{de_s^{ve}}{dt} = \sum_s \rho_s \frac{e_s^{ve*} - e_s^{ve}}{\tau_s} \tag{4}$$

where τ_s is the combined the Landau–Teller relaxation time. The Mutation++ library [29] (Multicomponent Thermodynamic And Transport properties for IONized gases in C++) provides algorithms for the computation of thermodynamic and chemical kinetic gas properties. SU2-NEMO code is coupled to this to provide capabilities to calculate combustion chemistry relevant to SFRJs.

To validate the computational framework, we consider the ramjet geometry considered in [30, 31]. The freestream pressure and temperature values are 30 kPa and 238 K, respectively. Figures 2 and 3, generated using the inviscid solver of SU2 [26], show the spatial distribution of the flow structures at a Mach 2.5 flow. In particular, Figure 2(a) shows the numerical density gradient magnitude. As can be seen, multiple oblique and bow shock interactions yield a complex flow structure, which, in turn, results in an increase in pressure and temperature values in the vicinity of the cowl, as shown in Figures 2(b) and (c), respectively. For an efficient combustion process, multiple shock reflections in the intake section yield a uniform flow field, especially downstream of the intake, as shown in Figure 2(d).

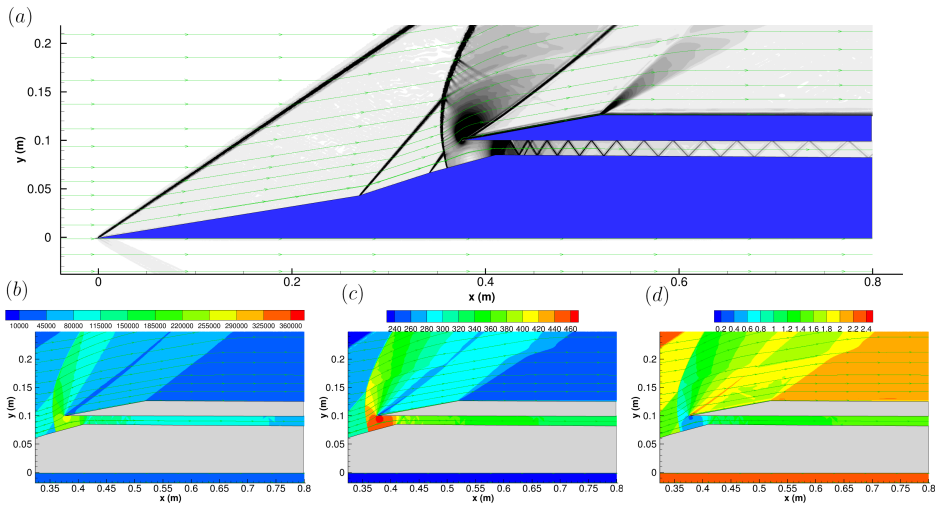

Fig. 2 Spatial distribution of the flow structures at Mach 2.5 flow. (a) **numerical Schlieren image constructed based on the density gradients of the simulation,** (b) **pressure field (Pa),** (c) **temperature field (K), and** (d) **Mach contours.**

The same flow conditions were simulated to investigate the impact of the presence of a bleed section and to control the mass flow rate using active and passive approaches. Figure 3 shows the spatial distribution of the flow field variables. A comparison between Figure 2 and 3 reveals that the extent of shock reflections diminishes significantly due to a relatively lower pressure difference associated with the presence of the bleed section. The interaction of multiple oblique shocks originating from the curvatures of the geometry results in higher temperatures upstream of the bleed. Additionally, the flow expands downstream of the bleed, resulting in higher Mach numbers as shown in Fig.3 (d).

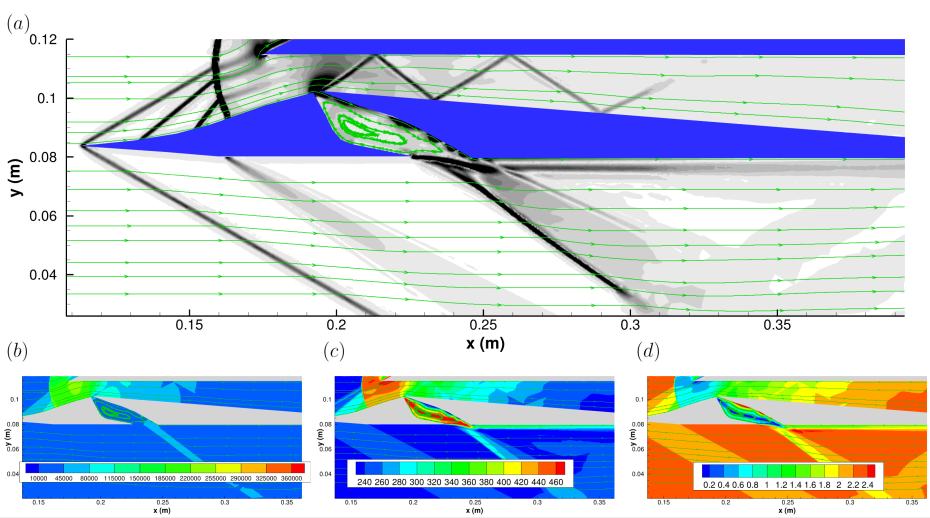

Fig. 3 Flow field parameters near an inlet with a bleed duct at Mach 2.5 flow. (a) **numerical Schlieren image constructed based on the density gradients of the simulation,** (b) **pressure field (Pa),** (c) **temperature field (K), and** (d) **Mach contours.**

In this work, to reduce the required computational resources, we consider a simplified geometry that is based on a 12-inch (0.3048 m) long cylinder with a diameter of 4 inches (0.1016 m). At the end of the cylinder is a diffuser whose length is 4 inches (0.1016 m) and exit diameter is 6 inches (0.1524 m). Since the cylinder is axis-symmetric about

the center line, only a two-dimensional cross-section of the cylinder is simulated. At the inlet of the cylinder, a total pressure of 30,000 Pa and a total temperature of 300 K is prescribed. Figure 4a shows the pressure field in the SFRJ in a steady-state condition. Figure 4b shows the steady-state thrust generated by the SFRJ for several constant heat flux values. Note the nonlinear input-output relation between the thrust and heat flux.

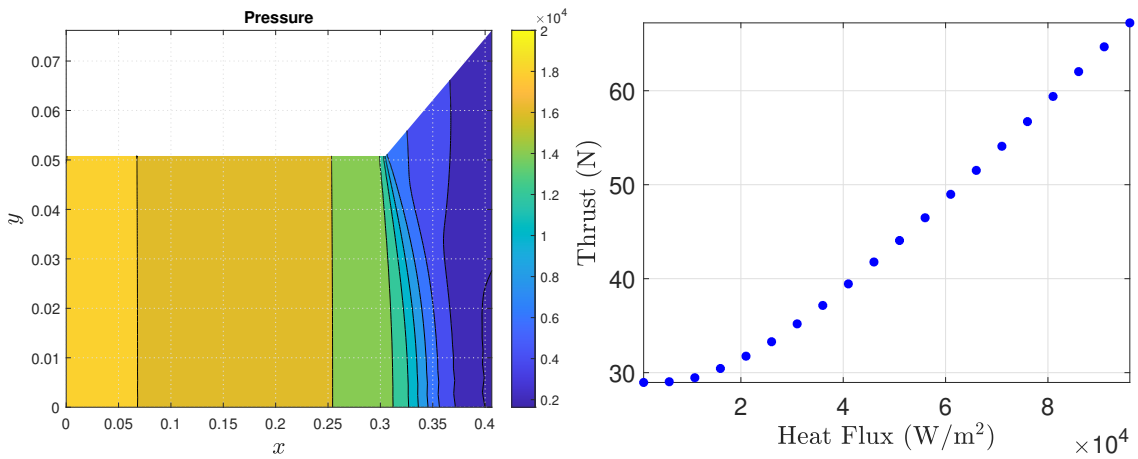

(a) Pressure field in the SFRJ in nominal steady-state conditions. **(b) Steady-state thrust generated by the SFRJ for several constant heat flux values.**

Fig. 4 Open-loop simulation of the SFRJ model.

III. Learning-based Thrust Regulation

This section describes the learning-based control system used to regulate the thrust generated by the SFRJ model described in the previous section. The closed-loop feedback control architecture is shown in Figure 5. The control system consists of an adaptive PI controller whose gains are optimized by the retrospective cost adaptive control (RCAC) algorithm and a nonlinearity that maps the RCAC output to the heat flux. The nonlinearity is chosen based on the open-loop simulations of the SFRJ model that showed the nonlinear relationship between the steady-state heat flux and the steady-state thrust output of the SFRJ.

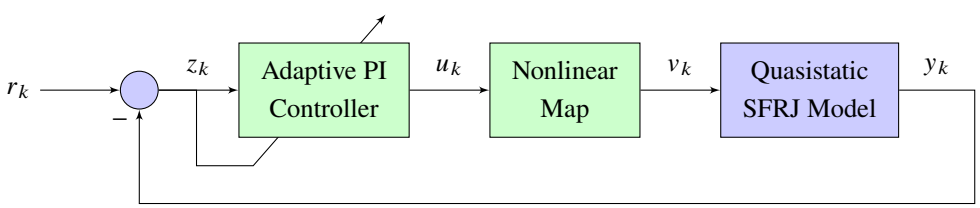

Fig. 5 Control architecture to regulate the thrust generated by the SFRJ.

The adaptive PI controller is given by

$$u_k = K_{\mathrm{P},k} z_k + K_{\mathrm{I},k} \gamma_k, \tag{5}$$

where z_k is the performance variable defined as the difference between the commanded thrust r_k and the measured thrust output y_k, that is, $z_k \triangleq r_k - y_k$, γ_k is the integrated performance variable given by

$$\gamma_k \triangleq \sum_{i=0}^{k} z_i, \tag{6}$$

and the scalars $K_{\mathrm{P},k}$ and $K_{\mathrm{I},k}$ are the proportional and integral gains optimized by the RCAC algorithm at step k. Note

that the integrated performance variable can be computed recursively as

$$\gamma_{k+1} = \gamma_k + z_{k+1}. \tag{7}$$

Note that the PI control law (5) can be written in the regressor form as

$$u_k = \Phi_k \theta_k, \tag{8}$$

where

$$\Phi_k \triangleq \begin{bmatrix} z_k & \gamma_k \end{bmatrix}, \quad \theta_k \triangleq \begin{bmatrix} K_{\mathrm{P},k} \\ K_{\mathrm{I},k} \end{bmatrix}, \tag{9}$$

where the regressor matrix Φ_k contains the measured data and the controller gain vector θ_k is optimized by the RCAC algorithm described in [32, 33]. Finally, the heat flux w_k is the output of a nonlinear map and is given by

$$w_k = w_0 + 10^{u_k}, \tag{10}$$

where w_0 is the nominal heat flux. Note that the units of the heat flux are $\mathrm{W/m^2}$.

The SFRJ is commanded to generate a constant thrust value of $r = 35$ N. In RCAC, we set $P_0 = 10^{-7} I_2, N_1 = 1$. Note that I_2 is the 2 identity matrix. The nominal heat flux $w_0 = 10000\ \mathrm{W/m^2}$. Figure 6 shows the closed-loop response. The first subplot shows the commanded and the generated thrust, the second subplot shows the control u_k given by RCAC, the third subplot shows the absolute value of the performance variable z_k on a log scale, and the fourth subplot shows the PI controller gains θ_k updated by RCAC at each step. Note that RCAC optimizes the controller coefficients using only the measured data and does not rely on the SFRJ model to optimize the controller.

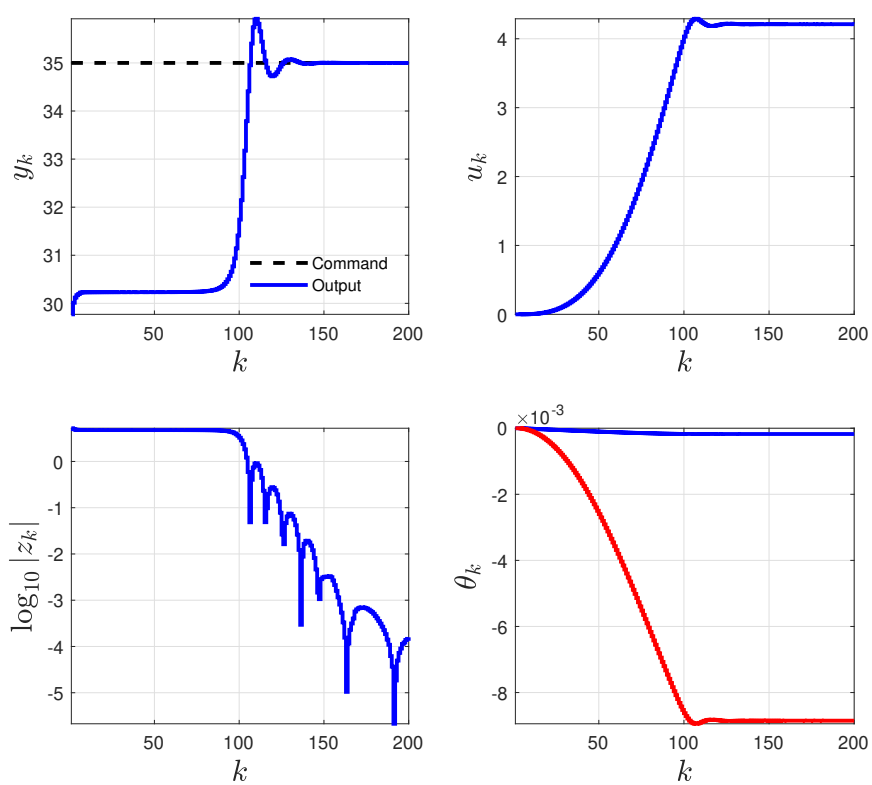

Fig. 6 Closed-loop response of the SFRJ to a step command

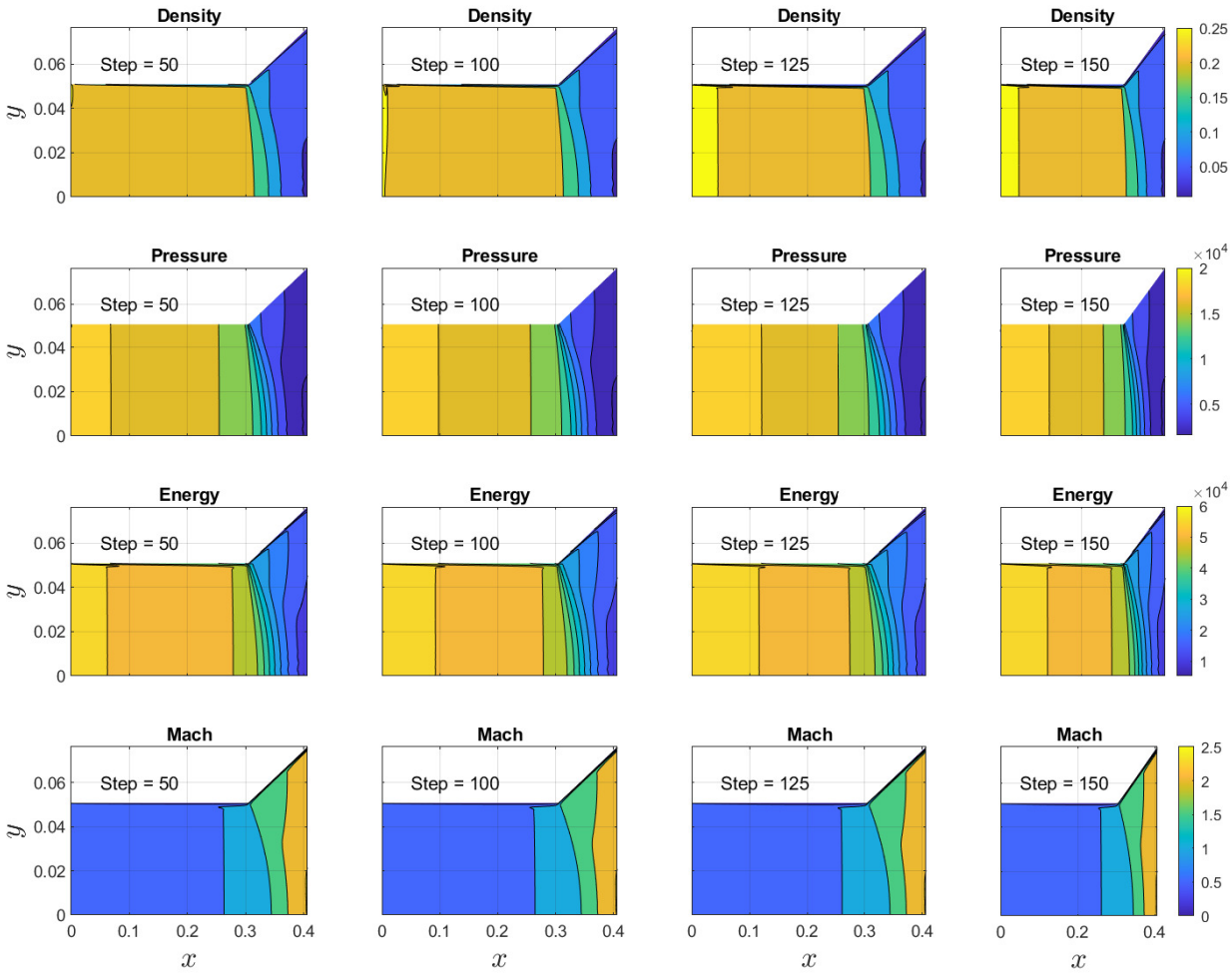

Fig. 7 Density, Pressure, Energy, and Mach number contour in the computational domain at various time steps.

Next, we investigate the performance of the adaptive controller in the case where reference commands are changed periodically. In RCAC, we set $P_0 = 10^{-7} I_2$, $R_u = 0$, $N_1 = 1$. Figure 8 shows the closed-loop response of the SFRJ to a sequence of step commands. The first subplot shows the commanded and the generated thrust, the second subplot shows the control u_k given by RCAC, the third subplot shows the absolute value of the performance variable z_k on a log scale, and the fourth subplot shows the PI controller gains θ_k updated by RCAC at each step. Note that the RCAC hyperparameters are not readjusted.

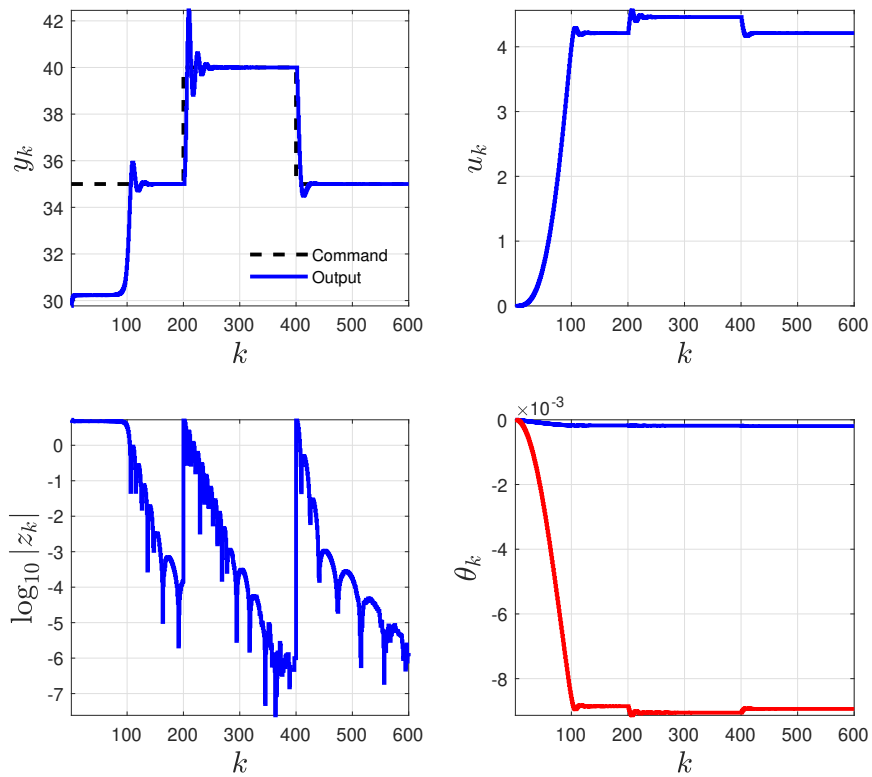

Fig. 8 Closed-loop response of the SFRJ to a sequence of step commands

Next, we investigate the effect of RCAC hyperparameters on the closed-loop performance. We reconsider the constant step command-following problem where $r_k = 35$ N. In RCAC, we set $N_1 = n$ and $P_0 = pI_2$, where $n = 0.1, 1, 10$ and $p = 10^{-6}, 10^{-7}, 10^{-8}$. Note that I_2 is the 2 identity matrix. The closed-loop simulation is thus run nine times with all combinations of n and p. Figure 9 shows the effect of RCAC hyperparameters on the closed-loop response of the SFRJ. The first subplot shows the thrust output y_k of the SFRJ, and the section subplot shows the control u_k used to generate the heat flux. Note that a larger value of P_0 yields faster convergence but results in a larger overshoot. Similarly, a larger value of N_1 yields a faster response.

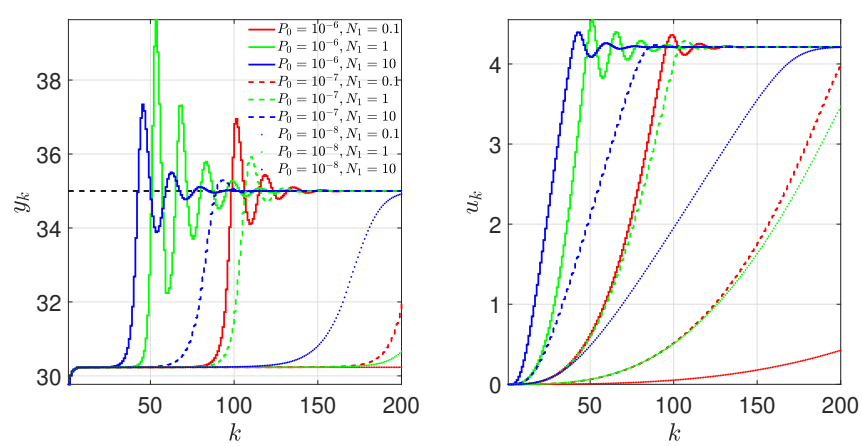

Fig. 9 Effect of RCAC hyperparameters P_0 and N_1 on the closed-loop response of the SFRJ.

IV. Conclusions

This paper presented the adaptive regulation of thrust generated by a solid fuel ramjet engine using a learning-based control technique. A quasi-static model of the solid fuel ramjet was simulated using the SU2-NEMO code with RANS fidelity. Open-loop simulations of the SFRJ model with various values of constant heat flux revealed a nonlinear relationship between the heat flux and the steady-state thrust output of the SFRJ. The adaptive control system, which consisted of a discrete-time, adaptive, proportional-integral controller, was thus augmented with a nonlinear map to prevent ill-conditioning of the optimization problem solved recursively in the adaptive controller. The gains of the PI controller were optimized using the retrospective cost adaptive control algorithm. The hyperparameters of the RCAC algorithm were tuned in a nominal simulation. The adaptive controller was then commanded to follow a sequence of step thrust commands without retuning. The effect of the hyperparameters of the RCAC algorithms on the convergence speed and settling time was investigated. To test the robustness of the adaptive controller, the Mach number at the inlet was varied without retuning the controller. In all scenarios, the adaptive controller followed the thrust command successfully. The future work will consider a more realistic heat addition mechanism and additional control variables, including bleed jets and variable bypass ratio.

V. Acknowledgment

This research was supported by the Office of Naval Research grant N00014-23-1-2468.

References

[1] Netzer, D. W., "Modeling solid-fuel ramjet combustion," *Journal of Spacecraft and Rockets*, Vol. 14, No. 12, 1977, pp. 762–766.

[2] Stevenson, C. A., and Netzer, D. W., "Primitive-variable model applications to solid-fuel ramjet combustion," *Journal of Spacecraft and Rockets*, Vol. 18, No. 1, 1981, pp. 89–94.

[3] Ben-Arosh, R., Natan, B., Spiegler, E., and Gany, A., "Theoretical study of a solid fuel scramjet combustor," *Acta Astronautica*, Vol. 45, No. 3, 1999, pp. 155–166.

[4] Sun, B., Wu, X. S., Cai, W. X., and Xia, Q., "Numerical Simulation of Pitot Solid Fuel Ramjets," *2009 International Conference on Computational Intelligence and Software Engineering*, 2009, pp. 1–4. https://doi.org/10.1109/CISE.2009.5365984.

[5] Wang, L., Wu, Z., Chi, H., Liu, C., Tao, H., and Wang, Q., "Numerical and experimental study on the solid-fuel scramjet combustor," *Journal of Propulsion and Power*, Vol. 31, No. 2, 2015, pp. 685–693.

[6] Schwer, D. A., O'Fallon Jr, E., and Kessler, D., "Liquid-fueled detonation modeling at the US Naval Research Laboratory," Tech. rep., Naval Research Lab Washington DC, 2018.

[7] Schwer, D. A., Johnson, R. F., Kercher, A., Kessler, D., and Corrigan, A. T., "Progress in efficient, high-fidelity, rotating detonation engine simulations," *AIAA Scitech 2019 Forum*, 2019, p. 2018.

[8] Kessler, D. A., Hess, A. M., Obenschain, K., Eder, D. C., Koniges, A., Knutson, A., Candler, G. V., Johnson, H., Starr, S., Bretheim, J., et al., "Performance of Coupled Physics Solvers for Multidisciplinary Hypersonic Flow Simulations on Several Classes of Computer Architectures," *AIAA SCITECH 2022 Forum*, 2022, p. 0973.

[9] Goodwin, G. B., Hyde, E. W., Bachman, C. L., Johnson, R. F., and Kessler, D. A., "Simulating Unstart in an Axisymmetric, Supersonic Cavity Flameholder," Tech. rep., Naval Research Lab Washington DC, 2022.

[10] Campbell Jr, W., Ko, B., Lowe, S., and Netzer, D., "Solid-fuel ramjet fuel regression rate/thrust modulation," *Journal of Propulsion and Power*, Vol. 8, No. 3, 1992, pp. 624–629.

[11] Pelosi-Pinhas, D., and Gany, A., "Bypass-regulated solid fuel ramjet combustor in variable flight conditions," *Journal of propulsion and power*, Vol. 19, No. 1, 2003, pp. 73–80.

[12] Pei, X., Wu, Z., Wei, Z., and Liu, J., "Numerical investigation on internal regressing shapes of solid-fuel scramjet combustor," *Journal of Propulsion and Power*, Vol. 29, No. 5, 2013, pp. 1041–1051.

[13] MacLeod, C., and Gerrard, C. E., "A review of air-fuel mixing and alternative methods in scramjets and scramjet-like engines." *Journal of the British Interplanetary Society*, Vol. 69, No. 4, 2016.

[14] Jarymowycz, T., Yang, V., and Kuo, K., "Numerical study of solid-fuel combustion under supersonic crossflows," *Journal of Propulsion and Power*, Vol. 8, No. 2, 1992, pp. 346–353.

[15] Durali, M., Alemohammad, S., and Alasty, A., "Propulsion control of a solid fuel ramjet using a robust adaptive neural controller," *Proceedings of 2005 IEEE Conference on Control Applications, 2005. CCA 2005.*, 2005, pp. 879–884. https://doi.org/10.1109/CCA.2005.1507240.

[16] Durali, M., and Alemohammad, H., "Velocity Regulation of a Solid Fuel Ramjet Using Neural Networks and Adaptive Sliding Control," *ASME International Mechanical Engineering Congress and Exposition*, Vol. 42169, 2005, pp. 239–248.

[17] Goel, A., Xie, A., Duraisamy, K., and Bernstein, D. S., "Retrospective cost adaptive thrust control of a 1D scramjet with Mach number disturbance," *2015 American Control Conference (ACC)*, 2015, pp. 5551–5556. https://doi.org/10.1109/ACC.2015.7172208.

[18] Goel, A., Duraisamy, K., and Bernstein, D. S., "Retrospective cost adaptive control of unstart in a model scramjet combustor," *AIAA Journal*, Vol. 56, No. 3, 2018, pp. 1085–1096.

[19] Goel, A., Duraisamy, K., and Bernstein, D., "Output-Constrained Adaptive Control for Unstart Prevention in a 2D Scramjet Combustor," *AIAA Scitech 2019 Forum*, 2019, p. 0927.

[20] Nusca, M. J., Chakravarthyt, S. R., and Goldberg, U. C., "Computational fluid dynamics capability for the solid-fuel ramjet projectile," *Journal of Propulsion*, Vol. 6, No. 3, 1990, pp. 256–262. https://doi.org/10.2514/3.25428.

[21] Gnoffo, P. A., "Planetary-Entry Gas Dynamics," *Annual Review of Fluid Mechanics*, Vol. 31, 1999. https://doi.org/10.1146/annurev.fluid.31.1.459.

[22] Candler, G. V., "Rate Effects in Hypersonic Flows," *Annual Review of Fluid Mechanics*, Vol. 51, No. 1, 2019, pp. 379–402. https://doi.org/10.1146/annurev-fluid-010518-040258, URL https://www.annualreviews.org/doi/10.1146/annurev-fluid-010518-040258.

[23] Josyula, E. (ed.), *Hypersonic Nonequilibrium Flows: Fundamentals and Recent Advances*, AIAA, 2015.

[24] Bertin, J. J., and Cummings, R. M., "Critical Hypersonic Aerothermodynamic Phenomena," *Annual Review of Fluid Mechanics*, Vol. 38, No. 1, 2006, pp. 129–157. https://doi.org/10.1146/annurev.fluid.38.050304.092041, URL http://www.annualreviews.org/doi/10.1146/annurev.fluid.38.050304.092041.

[25] Garbacz, C., Morgado, F., Fossati, M., Maier, W. T., Needels, J., Alonso, J. J., Capitelli, M., Scoggins, J. B., Magin, T. E., Liza, M., and Hanquist, K. M., "SU2-NEMO: An Open-Source Framework for Nonequilibrium Flows," *SU2 Conference 2021*, 2021. URL https://youtu.be/F1cua7NFId4.

[26] Economon, T. D., Palacios, F., Copeland, S. R., Lukaczyk, T. W., and Alonso, J. J., "SU2: An open-source suite for multiphysics simulation and design," *AIAA Journal*, Vol. 54, No. 3, 2016, pp. 828–846. https://doi.org/10.2514/1.J053813.

[27] Maier, W. T., Needels, J. T., Garbacz, C., Morgado, F., Alonso, J. J., and Fossati, M., "SU2-NEMO: An Open-Source Framework for High-Mach Nonequilibrium Multi-Species Flows," *Aerospace 2021, Vol. 8, Page 193*, Vol. 8, No. 7, 2021, p. 193. https://doi.org/10.3390/AEROSPACE8070193, URL https://www.mdpi.com/2226-4310/8/7/193/htmhttps://www.mdpi.com/2226-4310/8/7/193.

[28] Needels, J. T., Duzel, U., Hanquist, K. M., and Alonso, J. J., "Sensitivity Analysis of Gas-Surface Modeling in Nonequilibrium Flows," *AIAA SCITECH 2022 Forum*, AIAA Paper 2022-1636, 2022. https://doi.org/10.2514/6.2022-1636.

[29] Scoggins, J. B., Leroy, V., Bellas-Chatzigeorgis, G., Dias, B., and Magin, T. E., "Mutation++: MUlticomponent Thermodynamic And Transport properties for IONized gases in C++," *SoftwareX*, Vol. 12, 2020, p. 100575. https://doi.org/10.1016/j.softx.2020.100575.

[30] Gruhn, P., and Gülhan, A., "Experimental investigation of a hypersonic inlet with and without sidewall compression," *Journal of Propulsion and Power*, Vol. 27, No. 3, 2011, pp. 718–729.

[31] Krause, M., and Ballmann, J., "Numerical simulations and design of a scramjet intake using two different RANS solvers," *43rd AIAA/ASME/SAE/ASEE Joint Propulsion Conference & Exhibit*, 2007, p. 5423.

[32] Oveissi, P., Trivedi, A., Goel, A., Tumuklu, O., Hanquist, K. M., Farahmandi, A., and Philbrick, D., "Learning-based Adaptive Thrust Regulation of Solid Fuel Ramjet," *AIAA SCITECH 2023 Forum*, 2023, p. 2533.

[33] Poudel, N., Trivedi, A., Oveissi, P., Yu, M., Goel, A., and Hrynuk, J. T., "Learning-based Adaptive Gust Mitigation with Oscillating Wings," *AIAA SCITECH 2023 Forum*, 2023, p. 0275.